NUMERICAL INVESTIGATION OF COUNTER-FLOW PROCESSES IN GEOTHERMAL WELLS

Ryan Tonkin[1], John O'Sullivan[1], Michael O'Sullivan[1]

[1]Department of Engineering Science, University of Auckland, Auckland, New Zealand

rton671@aucklanduni.ac.nz

Keywords: *Transient, wellbore, simulation, counter flow, heat up*

ABSTRACT

One of the complex transient phenomena that can occur within geothermal wellbores is counter-flow. In geothermal wells, counter-flow occurs when steam flows up the well while water flows down. Here we discuss numerical experiments with a recently developed transient geothermal wellbore simulator that is capable of modelling counter-flow scenarios.

We use our simulator to investigate the role of counter-flow in two test cases involving shut-in geothermal wells. In the first test case, counter-flow occurs as a shallow geothermal well heats up and a vapour cap is formed. The results of this simulation suggest that the vapour cap develops because of the heat transport in a counter-flow zone that occurs in the two-phase fluid. For this reason, counter-flow processes cannot be ignored when simulating flow in a shut-in geothermal wellbore, even though the mass flows that occur during this process are small. A second test case simulates the opening of a multi-feed well to flow, starting with realistic shut-in initial conditions. These initial conditions, which were found using simulation, involve inter-zonal flow and counter-flow processes. They demonstrate that temperatures in the well differ from those in the reservoir when these processes occur. Additionally, this second test case highlights that counter-flow capabilities are required to fully model many transient wellbore processes, even something as fundamental as opening a well to flow.

The test cases show that simulation can be used to help in the interpretation of data from shut-in wells. However, the investigation shows that if a wellbore simulator is to be used in this capacity it must be able to model counter-flow processes.

1. INTRODUCTION

Wells are used to produce and re-inject geothermal fluid and provide important information for characterising the reservoir. However, complex processes that occur within a well can make the interpretation of wellbore behaviour difficult. Therefore, geothermal wellbore simulators are helpful in gaining insight into complex wellbore phenomena that are hard to observe.

One process of interest that can occur in a two-phase zone within a geothermal well is counter-flow (also called counter-current flow). It refers to cases in which the phases (water and steam) flow in opposite directions, i.e., when steam, the vapour phase, flows up the well while water, the liquid phase, flows down. This paper presents a preliminary investigation into the role of counter-flow processes in shut-in geothermal wellbores. The numerical modelling of shut-in wells is of interest because pressure and temperature data taken from these wells is used to infer reservoir characteristics that may be useful for calibrating numerical reservoir models (Grant and Bixley, 2011).

Our transient simulator is capable of modelling complex phenomena that occur in geothermal wells, including counter-flow. The theoretical background and numerical methods used in the simulator are presented elsewhere (Tonkin et al., 2020). When developing the simulator, we found that the formulation of the governing conservation equations, numerical methods (including the choice of primary variables), and the constitutive model for slip all affect the ability of the simulator to successfully model counter-flow. These factors are discussed in Section 2.

Section 3 presents Test Case 1, including a detailed discussion of the role of counter-flow processes within a shallow well as it heats up after a period of injection. Section 4 presents Test Case 2 with simulations of the opening of a shut-in multi-feed geothermal well. The initial conditions used for this case were found using simulation. The initial conditions used for Test Case 2 feature inter-zonal flow between the feed zones, counter-flow in the boiling region and a cold air cap.

2. MODELLING REQUIREMENTS FOR COUNTER-FLOW

It became clear when developing our simulator that not all geothermal wellbore simulators are capable of modelling counter-flow. For example, some commercial steady-state simulators such as WELLSIM (Hadgu, 1989; Gunn, 1990) and SWELFLO (McGuinness, 2015) cannot model counter-flow (or cases with zero mass flow). This is not an issue for these simulators as their intended use is for co-current production scenarios. However, as we wanted to develop a general transient simulator that could model general wellbore flow, including counter-flow and zero mass flow, we first investigated why some simulators could not model these types of flow. We found the formulation of the governing conservation equations, choice of primary variables, and the formulation of the constitutive model describing phase slip all impacted the ability of a simulator to model counter-flow. These factors are discussed below.

2.1 Formulation of the governing equations and primary variables

A geothermal wellbore simulator solves equations for the conservation of mass, momentum and energy. Formulating these equations in terms of variables weighted by mass flow is common, especially when modelling steady-state flows. Examples of variables

ISSN 2703-4275

weighted by mass flow include the flowing mass fraction, x_{fl} and x_{fv}, and the flowing mixture enthalpy, h_{fmix}. Numerical methods are used to solve the conservation equations for primary variables that describe the thermodynamic state of the well. When the conservation equations are formulated in terms of flowing variables, either the flowing vapour mass fraction or the flowing mixture enthalpy are chosen as a primary variable.

Using mass flow weighted variables when formulating or solving the governing conservation equations presents difficulties when attempting to model wells with zero mass flow or counter-flow. The reasons for this problem are discussed below, using the flowing mass fraction as an example. The same general argument applies to the flowing enthalpy as its definition, $h_{fmix} = x_{fv}h_v + x_{fl}h_l$, makes use of the flowing mass fractions.

The flowing mass fraction of phase β is defined as:

$$x_{f\beta} = Q_{m\beta}/Q_m \tag{1}$$

where, $Q_{m\beta}$ is the mass flow of phase β and the total mass flow is $Q_m = Q_{mv} + Q_{ml}$. This definition makes the flowing mass fraction a useful variable when simulating co-current flows. It allows the mass and volume flow of either phase to be calculated directly from the total mass flow (and pressure) and appears explicitly in many common slip relationships. Additionally, in geothermal applications, the flowing mass fraction is typically known (or is easily calculated) at the wellhead. However, as mentioned above, the definition in (1) is problematic when simulating general two-phase flow in wells. Table 1 gives the flowing vapour mass fraction for different flow scenarios that can occur within a well. The mass flow of each phase, total mass flow, saturation and flowing vapour mass fraction (calculated using (1)) are given for each case.

Table 1 indicates that when total mass flow equals zero, then x_{fv} is undefined. This situation can occur during counter-flow, when a well is shut-in or when the flow direction changes. Additionally, when general counter-flow occurs, in which the total mass flow does not necessarily equal zero, x_{fv} has a value outside the physical bounds for a mass fraction. Finally, the flowing mass fraction cannot differentiate between transitions from two-phase to single-phase conditions and transitions between the co-current and counter-flow regimes. The last two lines of Table 1 give the mass flow, vapour saturation and flowing mass fractions when the flow transitions between two-phase and single-phase conditions. Here, the mass flow of the disappearing phase (e.g., liquid when two-phase is transitioning to vapour) is zero. Comparing these cases with the conditions at the boundary between the counter-flow and co-current flow regimes, we see, for example, that x_{fv} has a value of one when transitioning between counter-flow and up-flow and when transitioning between two-phase and vapour conditions. This is because the liquid mass flow is zero in both cases. This means that x_{fv} does not uniquely define the transition to vapour conditions meaning that it should not be used for identifying phase transitions.

Given the issues with using the flowing mass fraction (or flowing enthalpy) as a primary variable, we decided that these variables should not be used when formulating or solving the governing conservation equations if counter-flow or zero-mass flow cases are of interest. As these cases can occur during transient wellbore flow, it seems better to use a variable such as vapour saturation. Table 1 indicates that vapour saturation stays within physical bounds for all cases and only takes a value of zero or one during transitions between two-phase and single-phase conditions.

Table 1: Flow scenarios that are possible during transient wellbore simulations and the corresponding mass flow rates, vapour saturation, S_v, and flowing vapour mass fraction, x_{fv} .

Flow scenario	Q_{mv}	Q_{ml}	Q_m	S_v	x_{fv}
Co-current up-flow	> 0	> 0	> 0	$0 < S_v < 1$	$0 < x_{fv} < 1$
Co-current down-flow	< 0	< 0	< 0	$0 < S_v < 1$	$0 < x_{fv} < 1$
Counter-flow	> 0	< 0	$Q_{ml} < Q_m < Q_{mv}$	$0 < S_v < 1$	$x_{fv} < 0$ or $x_{fv} > 1$
$Q_m = 0$ (e.g. stable counter-flow)	> 0	< 0	0	$0 < S_v < 1$	Undefined
Counter-flow/up-flow regime boundary	> 0	0	Q_{mv}	$0 < S_v < 1$	1
Counter-flow/down-flow regime boundary	0	< 0	Q_{ml}	$0 < S_v < 1$	0
Two-phase/vapour phase transition	$\neq 0$	0	Q_{mv}	1	1
Two-phase/liquid phase transition	0	$\neq 0$	Q_{ml}	0	0

2.2 Constitutive model for slip

As well as the three equations representing conservation of mass, momentum and energy, a transient geothermal wellbore simulator requires a constitutive model to describe phase slip. Common slip models such as those used by Hadgu (1989) (WELLSIM), Orkiszewski (1967), GWELL (Aunzo, 1991; McGuinness, 2015) and Duns and Ros (1963), are incapable of modelling counter-flow (McGuinness, 2015). Additionally, the Rouhani and Axelsson (1970) correlation, used in transient geothermal wellbore simulators developed by Garcia-Valladares et al. (2006) and Akbar et al. (2016), is a function of the flowing vapour mass fraction and therefore suffers from the problems discussed in Section 2.1 above for counter-flow processes.

ISSN 2703-4275

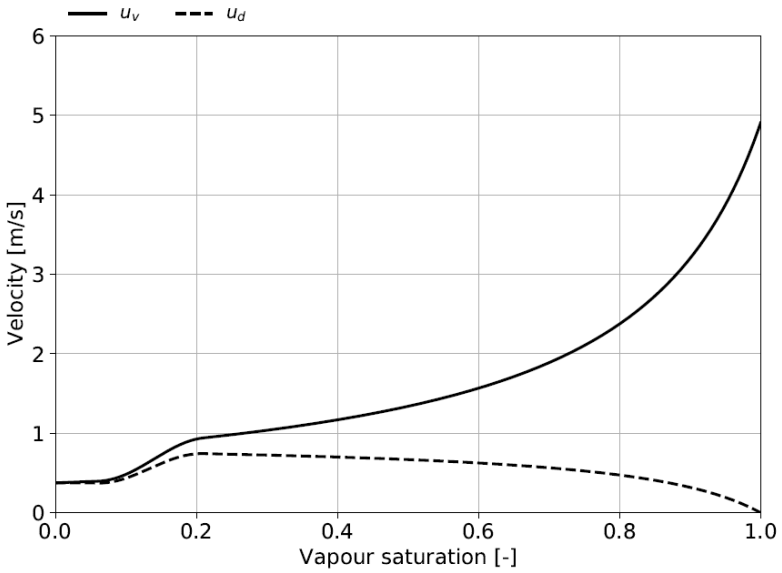

Figure 1: Shi et al.'s (2005) drift velocity, u_d, using Pan et al.'s (2011) smooth transition. The vapour velocity, u_v, is the minimum vapour velocity to prevent liquid downflow, representing the upper limit of the counter-flow regime.

Instead, we use a drift-flux model presented by Shi et al. (2005) to describe phase slip in our simulator. Their empirical relationships were optimised for use in deviated, wide diameter (15 cm) pipes using experimental data from Oddie et al. (2003). This makes their model well suited for geothermal applications. Additionally, our implementation of Shi et al.'s (2005) model is a function of vapour saturation and pressure, meaning that it does not suffer from the issues associated with the flowing mass fraction discussed in Section 2.1. Figure 1 shows this by plotting the upper limit of the counter-flow regime against vapour saturation using Shi et al.'s (2005) drift flux model. This regime boundary is defined as the minimum vapour velocity, u_v, required to prevent liquid down-flow.

Pan et al. (2011) used the drift-flux model of Shi et al. (2005) in their simulator T2WELL. However, they modified it to ensure that drift-flux parameters, namely the drift velocity and shape coefficient, were continuous and differentiable. We make use of this smooth transition, which is shown in Figure 1 by the smooth increase in the vapour and drift velocities between vapour saturations of 0.06 and 0.21.

3. TEST CASE 1: WELLBORE HEAT-UP

Test Case 1 models heat-up processes in a shallow geothermal well that has been closed after a period of injection. This test case was developed to investigate shut-in wellhead conditions and counter-flow processes within the well. It is, therefore, only 100 m deep with a constant diameter of 0.2 m and a completion diameter of 0.22 m. Additional model and simulation parameters are given in Table 2. The bottom boundary of the well is closed to flow, however, a source term in the bottom block allows fluid exchange with the reservoir. This vapour feed has a pressure of 20 bara, a temperature of 250 °C, and a productivity of 1E-6 kg/s/Pa. Finally, the formation temperature is assumed to be constant with time. It is shown in Figure 2 B).

This problem begins with the injection of 25 °C liquid water at a rate of 2 kg/s. Pressure, temperature and saturation conditions within the well after two days of injection are shown in Figure 2. These conditions correspond to a column of cold liquid water. After injecting liquid for two days, the wellhead is shut rapidly, and the well is left to heat up for 30 days. The counter-flow processes that occur as the well heats up and begins to boil are discussed in Section 3.1 below.

Table 2: Wellbore and simulation parameters for Test Case 1 modelling the heat-up of a shallow well.

Inclination angle	0 °
Length	100 m
Discretisation	Uniform, 200 blocks
Wellbore diameter	0.2 m
Cement diameter	0.22 m
Pipe roughness	4.5E-05 m
Wellhead boundary condition	Closed
Bottomhole boundary condition	Closed
Formation temperature	Figure 2 B)
Equation of state	Pure water
Heat flux model	Analytical – Ramey (1962)

ISSN 2703-4275

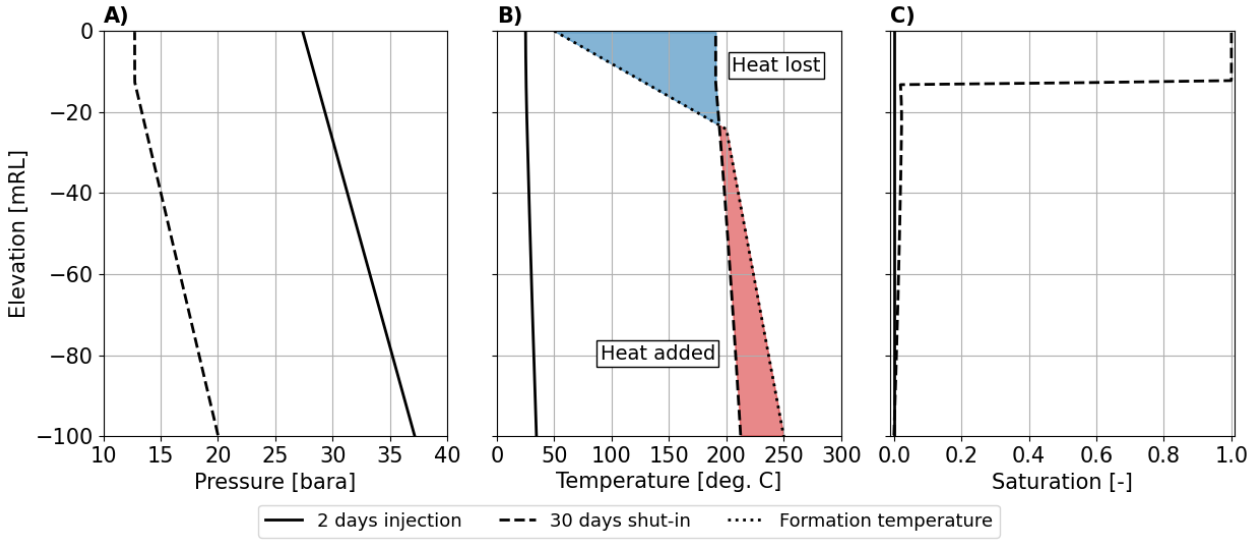

Figure 2: Wellbore conditions for Test Case 1 for A) pressure, B) temperature and C) vapour saturation after 2 days of injection and after 30 days of being shut-in.

3.1 Results and discussion

Figure 2 shows the pressure, temperature and saturation in the wellbore after two days of injection and at 30 days after shut-in. These profiles show that, after being shut in, the wellbore has heated up and a hot vapour zone has developed at the top of the well. The role of counter-flow in this process is discussed below using Figure 3, which plots the mass flows of each phase at various times. The saturation within the well is shown diagrammatically to the right of each mass flow plot in Figure 3.

Figure 3 A) plots the liquid and vapour mass flows 21 hours after shut-in. By this time, temperatures within the well have increased from the cold injection conditions shown in Figure 2 B) to saturation conditions, and boiling has just begun at the bottom of the well. At this stage, the liquid phase is flowing down the well and the vapour phase is bubbling up through the liquid.

Figure 3 B) shows that after seven more hours (approximately 28 hours after shut-in), boiling has progressed up the well to a depth of 12 m. Counter-flow is evident in the well below this point. Figure 3 B) shows that there is a net down-flow of fluid below 12 m, as the liquid down-flow is greater than the vapour up-flow. This is due to the two-phase fluid expanding as it boils, which increases wellbore pressures, forcing fluid down and out of the well. The counter-flow occurring below 12 m transports energy up the well, heating the liquid above the boiling zone. This is because the high enthalpy vapour phase transports more energy up the well than the lower enthalpy liquid phase transports down.

Figure 3 C) shows that boiling reaches the wellhead approximately three days and 22 hours after shut-in. Boiling takes longer to progress up this last 12 m of the well because, in this region, heat is lost to the formation due to its low temperature. This means the heating of the top 20 m is caused solely by the net upwards heat transfer that results from counter-flow.

After boiling reaches the wellhead, vapour begins to accumulate, causing a hot gas cap to form. Note that this gas cap is high saturation two-phase fluid rather than pure water vapour. As more vapour accumulates at the top of the well, the interface between the high and low saturation regions moves down the well. Physically, the liquid-dominated section below this interface has bubbles of vapour moving up through the water, which is balanced by a small downflow of liquid. The vapour boils off the top of the liquid-dominated column into the vapour-dominated zone. Here, the vapour slowly rises and loses heat to the formation. This heat loss causes some of the vapour to condense to liquid which flows back down the well.

Figure 3 D) shows that the well has reached steady-state conditions after being shut-in for 30 days. At this time, stable counter-flow occurs at all depths. Here, the vapour up-flow is equal in magnitude and opposite in direction to the liquid down-flow, and mass flow to the feed is zero. This is required to satisfy mass conservation for a shut-in single-feed well. Figure 2 C) shows that the hot vapour cap has developed in the top 12.5 m of the well. Comparing the temperature profile at 30 days with the formation temperature in Figure 2 B) indicates that the processes occurring within the well are driven by heat transfer between the wellbore and the formation. In this case, the well is essentially acting as a long heat exchanger. Heat is added to the well in the region highlighted in red in Figure 2 B). Counter-flow processes transport heat up the well where it is lost to the formation in the area highlighted in blue.

The results of this simulation show that counter-flow processes start as soon as boiling begins in the well. They suggest that the vapour cap that can exist in a geothermal well develops because of convective heat transport due to counter-flow that occurs in the two-phase fluid. For this reason, counter-flow processes cannot be ignored when simulating the shutting-in of a geothermal wellbore, even though the mass flows that occur during this process are small.

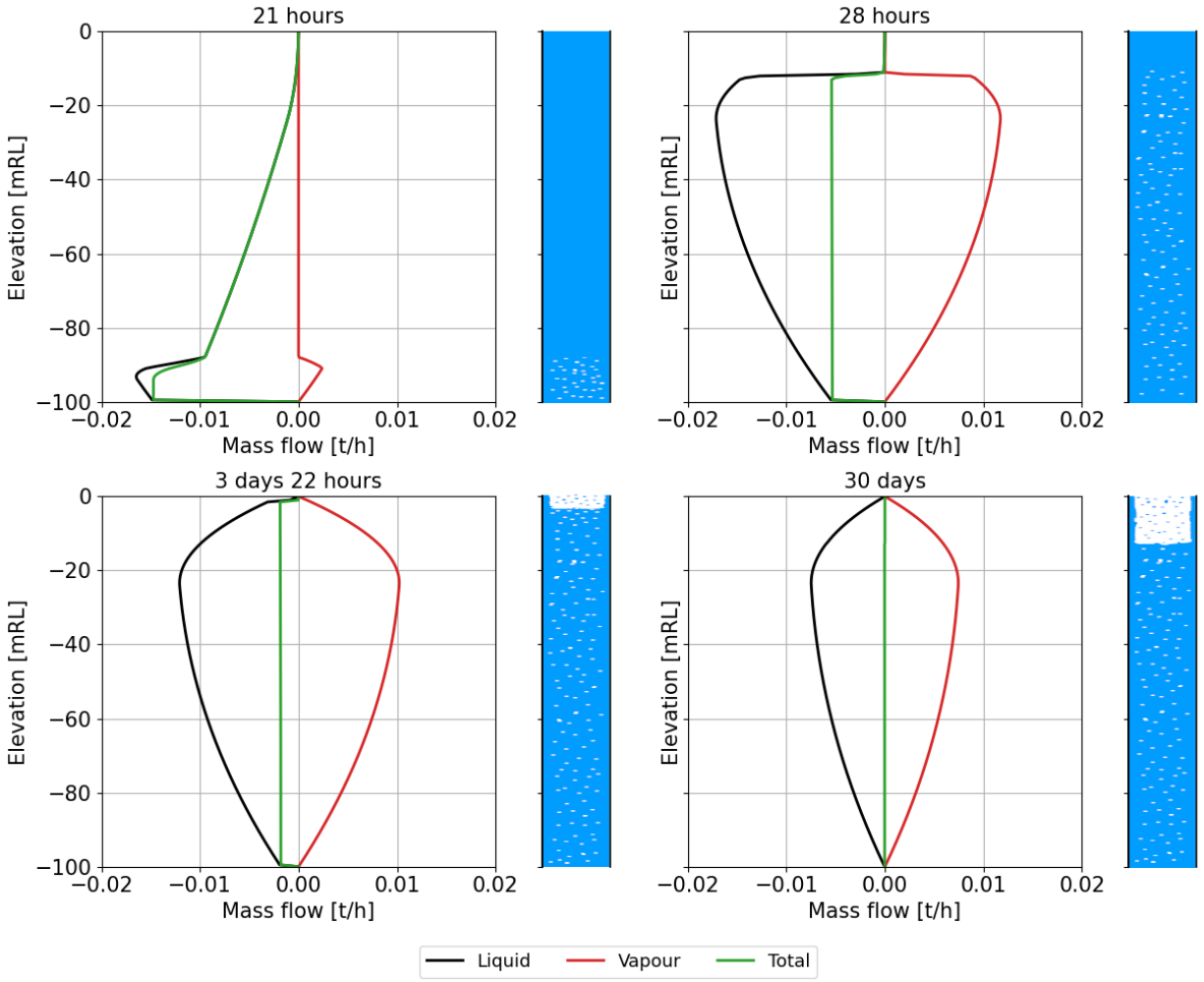

Figure 3: Plots of the liquid, vapour, and total mass flow A) 21 hours, B) 28 hours, C) three days and 22 hours and D) 30 days after shut-in for Test Case 1. These plots show that counter-flow is occurring within the well as it heats up. The corresponding wellbore saturation is shown diagrammatically to the right of each mass flow plot.

Table 3: Wellbore and simulation parameters for Test Case 2.

Inclination angle	0 °
Length	1000 m
Discretisation	Uniform, 200 blocks
Wellbore diameter	0.2205 m above -660 mRL
	0.16 m below -660 mRL
Cement diameter	0.314 m above -660 mRL
	0.17 m below -660 mRL
Pipe roughness	4.5E-05 m above -660 mRL
	9.0E-05 m below -660 mRL
Bottomhole boundary condition	Closed
Feed zone properties	Table 4
Formation temperature	Figure 4 B)
Equation of state	Air-water
Heat flux model	Analytical – Ramey (1962)

Table 4: Feed-zone properties for Test Case 2.

Feed location	Elevation [mRL]	α [kg/s/Pa]	P [bara]	h_{fmix} [kJ/kg]
Middle	-490 to -500	8.3e-07	33.00	1034
Deep	-990 to -1000	8.3e-07	66.82	1251

ISSN 2703-4275

4. TEST CASE 2: OPENING A WELL TO FLOW

Test Case 2 demonstrates that the counter-flow processes discussed in Section 3 also occur in more complex, more realistic wells. Test Case 2 simulates flow in a 1000 m well with a diameter of 0.2205 m above -660 mRL. The diameter decreases to 0.16 m below -660 mRL. Other model and simulation parameters are given in Table 3. The formation temperature profile for this test case is shown in Figure 4 B). It has a linear transition from 25 °C to 100 °C over the first 100 m. Below this point, the formation temperatures follow the boiling point for depth profile. This well has two feed-zones that allow transfer of mass and energy to and from the reservoir. The properties of each feed are given in Table 4.

Figures 4 and 5 show the wellbore conditions 30 days after being shut-in. These conditions were simulated by shutting the wellhead after a period of cold water injection. For this well, the wellhead pressure drops below atmospheric conditions after shut-in. In this case, air is allowed into the well so that the water level can drop. We use a "one-way" feed located in the top block of the model to control the flow of air into and out of the well. This feed allows air into the well when the wellhead pressure drops below atmospheric pressure. When the wellhead pressure increases above atmospheric conditions (i.e., when boiling begins to occur), the feed does not accept fluid, which allows the well to pressurise. The use of this feed and the simulation of realistic initial conditions for geothermal wellbores is discussed in more detail in a companion paper (Tonkin et al., 2021).

The shut-in conditions for this test case show several interesting features. Firstly, inter-zonal flow occurs between the two feeds. Figure 5 A) indicates that fluid enters the well at -500 mRL at approximately 230 °C. It flows down the well at 0.8 t/h and exits via the deep feed at the same rate. This down-flow is evident in the near-isothermal temperature profile for the bottom 500 m of the well, shown in Figure 4 B). Secondly, boiling occurs in the well between -20 and -500 mRL. Figure 5 B) shows that counter-flow occurs in this section of the well. The comparison of the well and formation temperatures in Figure 4 B) indicates that, in this case, the isothermal temperatures between -30 and -200 mRL do not reflect the reservoir temperatures. The high saturation two-phase column is caused by boiling in the wellbore and the heat transfer resulting from counter flow, as discussed in Section 3. Similarly, the non-isothermal temperatures between -200 mRL and -500 mRL do not reflect the reservoir temperatures. Differences range from approximately 2 °C at -500 mRL to approximately 15 °C at -200 mRL. Finally, Figure 4 C) indicates that the top 30 m of the well is occupied by air, which was drawn into the well after shut-in. There is no circulation or counter-flow in this section of the well. As a result, there is no energy transport from the hotter region of the well, and therefore this section of the well is at reservoir temperatures.

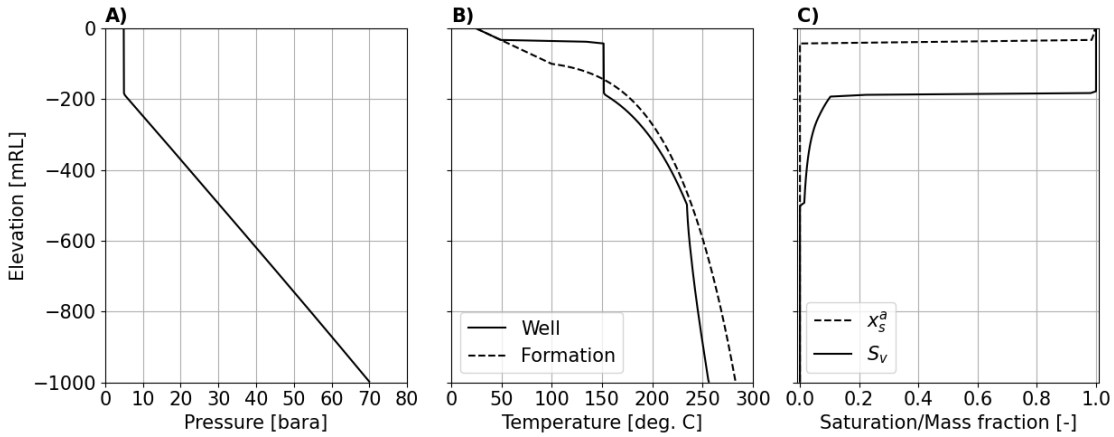

Figure 4: Plots of the initial conditions for the wellbore described in Section 4.1. A) pressure vs elevation, B) wellbore and formation temperature vs elevation, C) vapour and air mass fractions vs elevation after 30 days of heat-up.

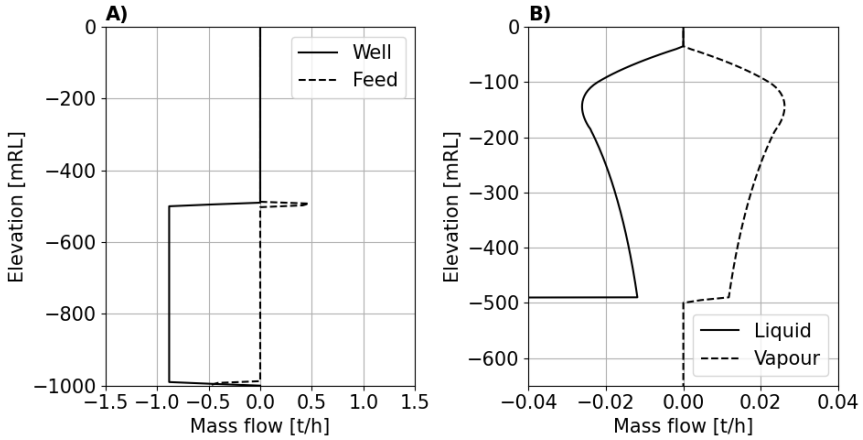

Figure 5: A) total mass flow rate within the well, showing inter-zonal flow. B) mass flow rates for the liquid and vapour phases between 0 – 600 m, showing counter-flow exists in the well after 30 days of heat-up.

ISSN 2703-4275

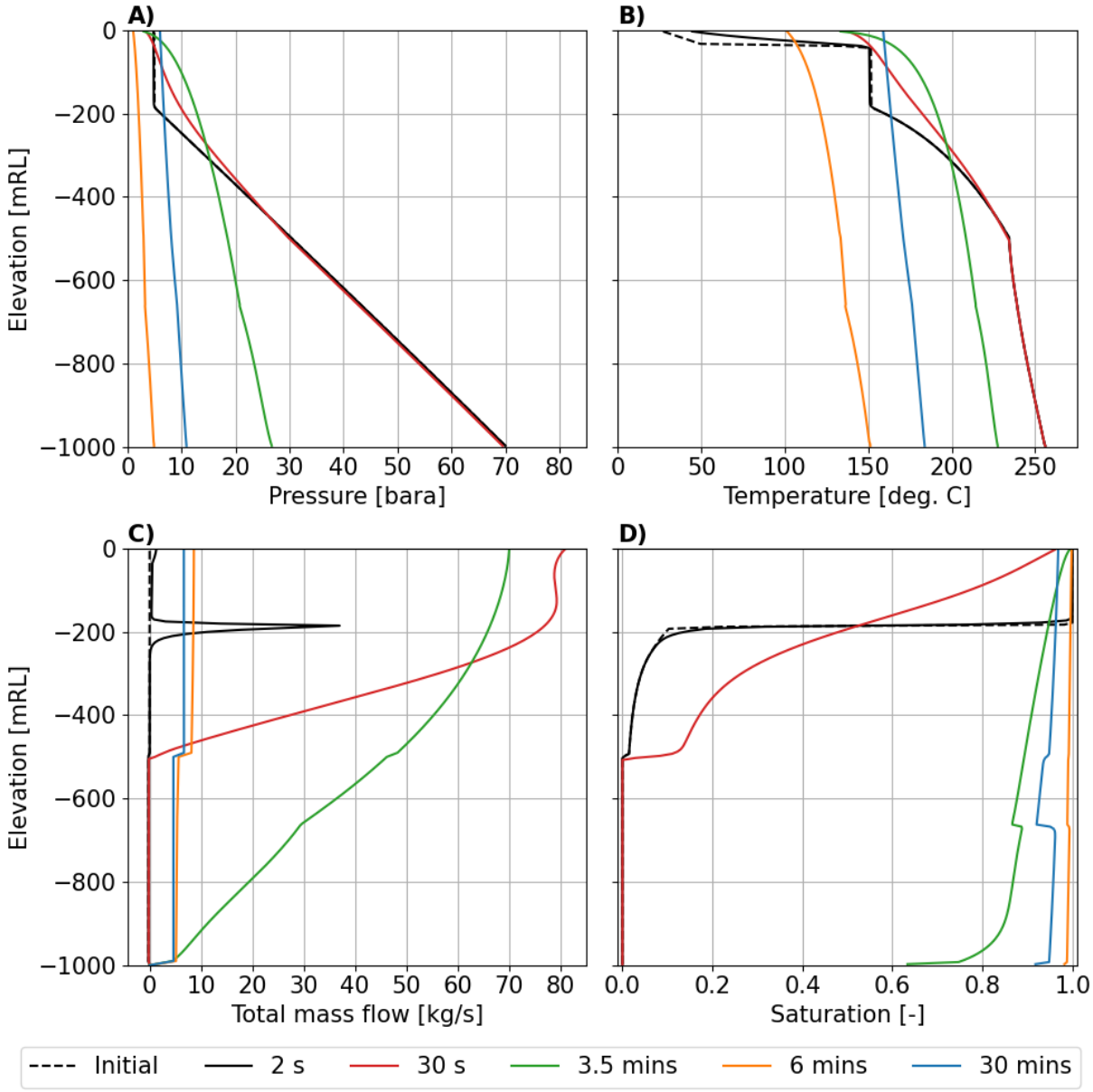

Figure 6: Profiles of A) pressure, B) temperature, C) total mass flow and D) vapour saturation as the well described in Section 4 is opened to flow.

Boiling that occurs while this well is shut-in causes the wellhead pressure to increase to approximately 5.0 bara from atmospheric conditions. This over-pressure makes it possible to start the well by simply opening the wellhead. Figure 6 shows how this process evolves with time. The well is opened to flow by dropping the wellhead pressure from 5.0 bara to 1.01325 bara over 60 seconds. The depressurisation of the well causes rapid flashing processes to occur at -200 mRL. The two-phase fluid expands as it flashes, resulting in the rapid increase in mass flow at -200 mRL that is shown in Figure 6 C). After 30 seconds, vapour saturation has increased between -200 and -500 mRL as hot fluid is transported up the well. The production of hot two-phase fluid causes the wellhead temperature to increase from 25 °C to 130 °C during this 30 second period. After 3.5 minutes, the flashpoint has reached the bottom of the well. This flashing causes the average density of the fluid to decrease, which results in a significant drop in pressure deep in the well. This pressure drop causes hot geothermal fluid to be produced from both feeds. After 5 minutes, we start slowly increasing the wellhead pressure to an operating pressure of 6.0 bara. This simulates switching production from a silencer at atmospheric conditions to the surface network at the separator pressure. After 30 minutes, production from the well has stabilised and reached operating conditions.

Test Case 2 highlights that a simulator requires counter-flow capabilities to completely model even the most fundamental wellbore processes, in this case, opening a well to flow. Additionally, the initial conditions used for Test Case 2, which were found using simulation, highlight some of the difficulties faced when interpreting shut-in data from hot geothermal wells. We suggest that simulation of shut-in wells could be used to aid and confirm the interpretation of this data.

5. CONCLUSIONS

This paper discusses modelling counter-flow in shut-in geothermal wells, a process that not all geothermal wellbore simulators can model. One of the reasons that some simulators are not suitable for counter-flow cases is that they use variables weighted by mass flow, such as flowing mass fractions and the flowing enthalpy, when formulating and solving the governing equations. We suggest that these variables should be avoided if counter-flow processes are to be simulated.

We used our transient wellbore simulator to study counter-flow processes that occur within shut-in geothermal wells. Test Case 1 studied a shallow geothermal well while it heated up. Counter-flow processes occurred as soon as boiling began at the bottom of the well. The resulting energy transport heated the top section of the well and caused a hot vapour cap to form. Counter-flow played the same role in Test Case 2, which modelled the opening of a multi-feed well. We conclude that shut-in conditions for geothermal wells with boiling cannot be modelled accurately without modelling counter-flow, even though small mass flows occur during this process.

Currently, pressure and temperature data from shut-in wells is interpreted manually using the expertise of experienced reservoir engineers to gain information about the characteristics of the reservoir. This information may also be used to calibrate numerical reservoir models. Processes such as boiling in the wellbore and inter-zonal flow, which were demonstrated in Test Case 2, can obscure reservoir temperatures and present difficulties when analysing wellbore data. We suggest that wellbore simulation should be used to aid and confirm the interpretation of shut-in wellbores. This investigation indicates that if a wellbore simulator is to be used in this capacity, it must be able to simulate counter-flow processes.

REFERENCES

Akbar, S., Fathianpour, N. and Al-Khoury, R.: A Finite Element Model for High Enthalpy Two-Phase Flow in Geothermal Wellbores, *Renewable Energy* **94**, 223–236. (2016).

Aunzo, Z. P., Bjornsson, G. and Bodvarsson, G. S. *Wellbore Models GWELL, GWNACL, and HOLA User's Guide*. California. (1991).

Duns, H. and Ros, N.C.J.: Vertical flow of gas and liquid mixtures in wells, *6th World Petroleum Congress*, 451–465. (1963).

García-Valladares, O., Sánchez-Upton, P. and Santoyo, E.: Numerical Modeling of Flow Processes Inside Geothermal Wells: An Approach for Predicting Production Characteristics with Uncertainties, *Energy Conversion and Management*, (2006).

Grant, M.A. and Bixley, P.F.: *Geothermal Reservoir Engineering*. Second Edition. Academic Press. (2011).

Gunn, C.: *Aspects of Geothermal Wellbore Simulation*. The University of Auckland. (1992)

Hadgu, T.: *Vertical Two-phase Flow Studies and Modelling of Flow in Geothermal Wells*. The University of Auckland. (1989)

Mcguinness, M.J.: *SwelFlo User Manual*. Wellington. (2015)

Oddie, G., Shi. H., Durlofsky, L.J., Aziz, K., Pfeffer, B. and Holmes, J.A.: Experimental study of two and three phase flows in large diameter inclined pipes, *International Journal of Multiphase Flow* **29**(4), 527–558. (2003).

Orkiszewski, J.: Predicting Two-Phase Pressure Drops in Vertical Pipe, *Journal of Petroleum Technology* **19**(6). (1967).

Pan, L., Oldenburg, C.M., Wu, Y.S. and Pruess, K.: *T2Well/ECO2N Version 1.0: Multiphase and Non-Isothermal Model for Coupled Wellbore-Reservoir Flow of Carbon Dioxide and Variable Salinity Water*, Technical report, Lawrence Berkeley National Laboratory. (2011).

Ramey, H. J.: Wellbore Heat Transmission, *Journal of Petroleum Technology* **14**(04), 427–435. (1962).

Rouhani, S. Z. and Axelsson, E.: Calculation of void volume fraction in the subcooled and quality boiling regions, *International Journal of Heat and Mass Transfer* **13**(2), 383–393. (1970).

Shi, H., Holmes, J. A., Durlofsky, L. J., Aziz, K., Diaz, L. R., Alkaya, B. and Oddie, G.: Drift-Flux Modeling of Two-Phase Flow in Wellbores, *SPE Journal* **10**(01), 24–33. (2005).

Tonkin, R. O'Sullivan, J. and O'Sullivan, M.: Development of a transient, multi-feed geothermal wellbore simulator. *Proc. 42nd New Zealand Geothermal Workshop*, Waitangi, NZ. (2020).

Tonkin, R. O'Sullivan, J. and O'Sullivan, M.: Modelling Discharge Stimulation Using a Transient Wellbore Simulator with an Air-Water Equation of State. *Proc. 43nd New Zealand Geothermal Workshop*, Wellington, NZ. (2021).

ISSN 2703-4275